ACS APPLIED MATERIALS & INTERFACES

Letter

www.acsami.org

Self-Templated Synthesis of Mesoporous Carbon from Carbon Tetrachloride Precursor for Supercapacitor Electrodes

Duihai Tang, Shi Hu, Fang Dai, Ran Yi, Mikhail L. Gordin, Shuru Chen, Jiangxuan Song, and Donghai Wang*

Department of Mechanical and Nuclear Engineering, The Pennsylvania State University, University Park, Pennsylvania 16802, United States

Supporting Information

ABSTRACT: A high-surface-area mesoporous carbon material has been synthesized using a self-templating approach via reduction of carbon tetrachloride by sodium potassium alloy. The advantage is the reduction-generated salt templates can be easily removed with just water. The produced mesoporous carbon has a high surface area and a narrow pore size distribution. When used as a supercapacitor electrode, this material exhibits a high specific capacitance (259 F g^{-1}) and excellent cycling performance (>92% capacitance retention for 6000 cycles).

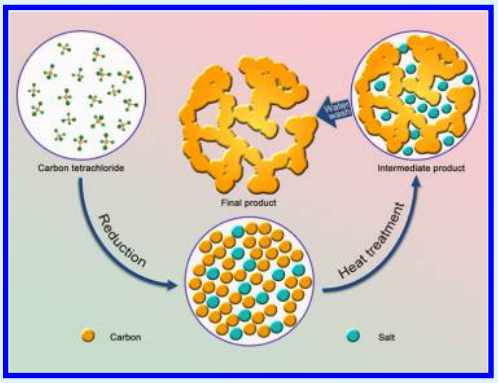

KEYWORDS: *mesoporous carbon, self-templating, carbon tetrachloride, sodium potassium alloy, supercapacitor*

Mesoporous carbon materials are of interest in many applications thanks to their high surface area and favorable physicochemical properties,[1] including electrical conductivity, thermal conductivity, chemical stability, and mechanical stability.[2] They have been widely applied in gas storage, water purification, catalyst supports, and electrode materials for fuel cells, batteries, and supercapacitors[3] The preparation of mesoporous carbon usually involves high-temperature pyrolysis of organic precursors with different types of templates. A wide variety of precursors have been used to prepare the mesoporous carbon.[4] In 1999, Ryoo's group reported the preparation of ordered mesoporous carbon by carbonization of sucrose inside mesoporous silica template. The mesoporous carbon could be obtained after the removal of the silica template by using sodium hydroxide aqueous solution.[5] Since then, many other organic precursors have been utilized, including petroleum pitches,[6] resins (phenol-formaldehyde and resorcinol-formaldehyde resins),[7] alkene (ethylene and propylene),[8,9] aromatic precursors (naphthalene, anthracene, pyrene, benzene, styrene, and acenaphthene),[10,11] and other small organic molecules (furfuryl alcohol and acetonitrile).[12] Carbon tetrachloride (CCl_4) has also been used as precursor for preparation of nonporous carbon material. For example, Li and Qian reported synthesis of diamond through the reaction between CCl_4 and sodium at 700 °C.[13] Numerous research works have subsequently been conducted focusing on the reactions of alkali metals and halocarbon to produce carbon materials.[14−16]

As to the templates for the synthesis of the mesoporous carbon, there are two major categories: supramolecular aggregates such as surfactant micelle arrays (soft template) and preformed mesoporous solids (hard template) such as SiO_2, $CaCO_3$, and MgO.[17−19] In the synthesis, the organic precursors are directed into organized structure by the templates, carbonized at high temperature, and then the templates are completely removed by chemical (leaching, etching) or physical (thermal treatment) methods to obtain the mesoporous carbon.[20] Additionally, some activation-free strategies have also been developed to synthesize porous carbon.[21,22] However, the template-free methods to synthesize mesoporous carbon are rarely reported and thus desirable.

In this report, we introduce a new synthesis procedure of mesoporous carbon without any external templates. The mesoporous structure is generated by a self-templating method using reaction byproducts as templates and carbon tetrachloride as precursors. The synthesis is via reduction of liquid carbon tetrachloride by sodium potassium alloy (NaK, liquid) and self-assembly of the reduction-generated carbon atoms around the as-generated salt byproduct.[23] The advantage is the reduction-generated salt templates can be easily removed with just water. The produced mesoporous carbon has a high Brunauer−Emmett−Teller (BET) surface area of 2012 m^2 g^{-1} and a narrow pore size distribution, with an average pore diameter of

Received: December 14, 2015
Accepted: February 25, 2016
Published: February 25, 2016

DOI: 10.1021/acsami.5b12164
ACS Appl. Mater. Interfaces 2016, 8, 6779−6783

4 nm. Benefiting from its high surface area and mesoporous structure, the mesoporous carbon was evaluated as an electrode material for supercapacitors and exhibits high specific capacitance (259 F g^{-1} at 1 A g^{-1}), and high rate stability (189 F g^{-1} at a higher current density of 100 A g^{-1}).

The preparation of this mesoporous carbon was carried out in a glovebox filled with Ar (see details in Supporting Information). The synthetic route is schematically shown in Figure 1 NaK alloy was slowly added to a toluene solution of

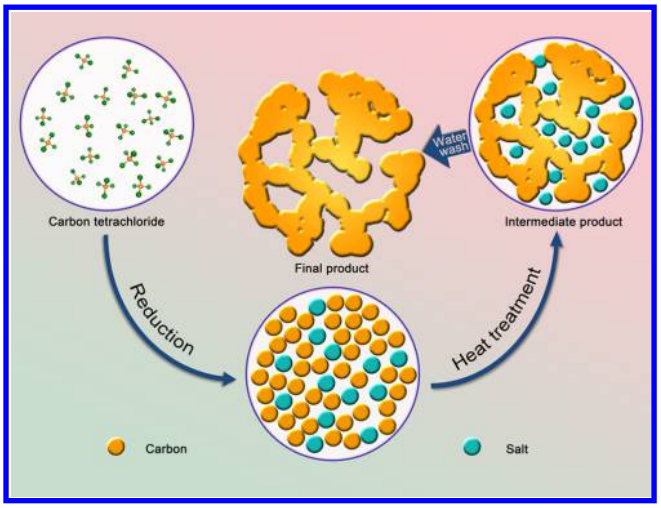

Figure 1. Synthetic route of the mesoporous carbon.

carbon tetrachloride (CCl_4) by syringe. This mixed solution was vigorously stirred and heated at 120 °C for 8 h, with the production of black particles. Then hydrogen chloride solution (2 M in diethyl ether) was added slowly into the mixture. The intermediate products were collected and carbonized at 700 °C (heated up at the rate of 15 °C min^{-1}) for 40 min under Ar flow. These products were washed with excess DI water, and collected by filtration. Finally, the as-prepared mesoporous materials were dried at 80 °C under vacuum for 12 h before use. These mesoporous materials were named as MC.

X-ray powder diffraction (XRD) pattern of MC is shown in Figure 2a. The broad and low intensity diffraction peaks at 26.3° and 43.8° indicate the low degree of graphitization and amorphous nature of the final product.[24] The Raman spectrum of the final product (Figure 2b) has two broad peaks at around 1330 and 1600 cm^{-1}, which correspond to the D-band and the G-band, respectively. The higher intensity of the D band compared to the G band further proves the disordered atomic structure of MC.[25]

Nitrogen adsorption/desorption isotherm (Figure 3a) confirms the mesoporous structure of MC. The BET specific surface area of MC reaches 2012 m^2 g^{-1}, and the pore volume of MC is 2.35 cm^3 g^{-1}. Besides, this material has a narrow pore size distribution with an average pore diameter of 4−5 nm (Figure 3b), as calculated by Barrett−Joyner−Halenda (BJH) method. In contrast, the intermediate products have a BET surface area of 40 m^2 g^{-1} (as shown in Figure S1), which is much smaller than that of the final product MC. This result confirms that the KCl and NaCl salts formed during the reduction serve as templates for the formation of the pores.

The intermediate product obtained after precursor reduction was collected and characterized in order to confirm our proposed reaction mechanism. The XRD pattern of the

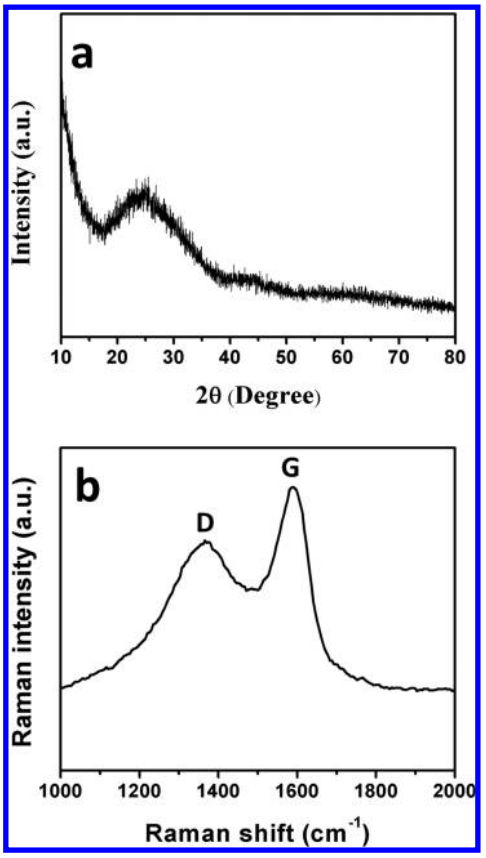

Figure 2. (a) XRD pattern of MC and (b) Raman spectrum of MC.

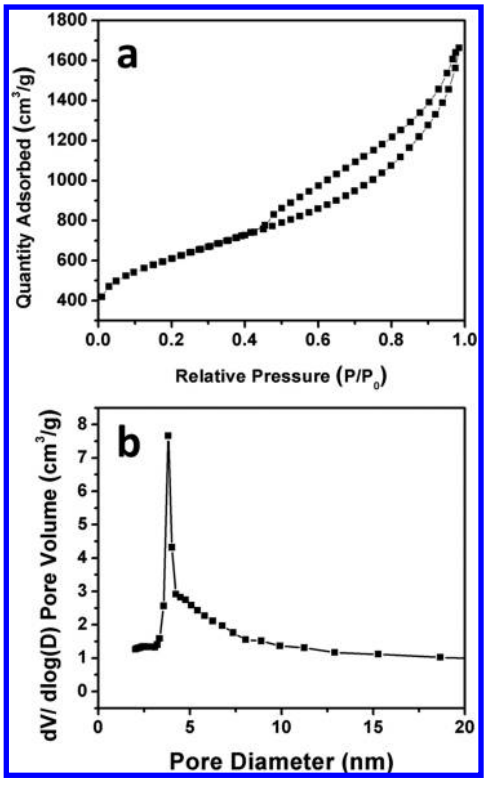

Figure 3. (a) Nitrogen-sorption isotherm and (b) BJH pore-size distribution of MC.

intermediate product (Figure S2) suggests the formation of salts of NaCl and KCl. The TEM images of the intermediate

DOI: 10.1021/acsami.5b12164
ACS Appl. Mater. Interfaces 2016, 8, 6779−6783

product (Figure 4a, b) show that the KCl nanocrystals with diameter of 5−10 nm are observed within the carbon matrix,

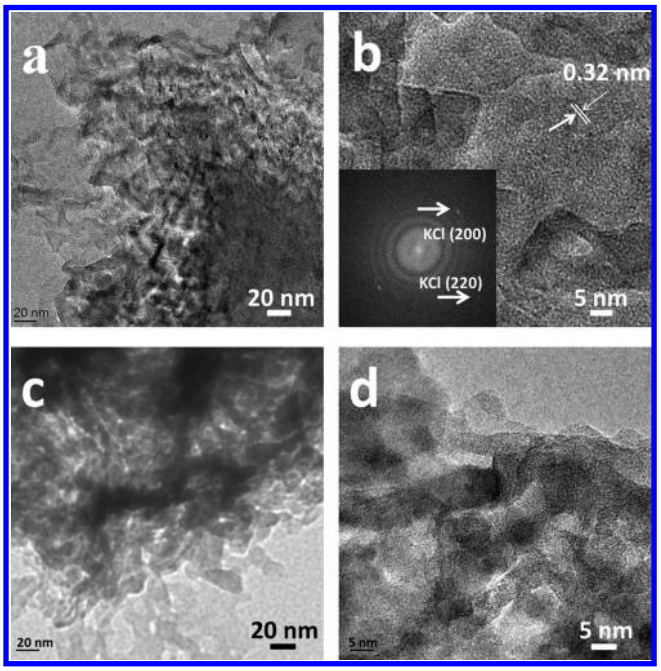

Figure 4. (a) Low-magnification TEM image of the intermediate products, (b) HRTEM image of the intermediate products, (c) low-magnification TEM image of MC, and (d) HRTEM image of MC.

and the lattice fringes of KCl [200] with a *d*-spacing of 0.32 nm are also clearly shown in the HRTEM image (Figure 4b). The crystallite size of the salt is similar as the pore size of MC. The SEM (Figure S4) and TEM images of MC (Figure 4c, d) show typical morphology of MC with a disordered mesoporous structure. Moreover, in Figure 4d, there are no salts left in this mesoporous material. According to the XRD patterns, the BET results and the TEM images, the self-forming templates could be removed totally with just water.

A mechanism of the synthesis procedure is proposed based on the results described above. In the first step, both salts (KCl and NaCl) and carbon are produced and precipitated by the reduction of CCl_4 because of the low solubility of the salts in toluene, as well as the fast production of large quantity of the intermediate products (salts and carbon). Second, the precipitation process and the aggregation process can lead to formation of the intermediate product where the as-generated salts aggregate and assemble with the reduction-generated carbon into a composite. Finally, in the heat treatment, the salt byproducts act as the template for the formation of mesoporous structure in the carbon. After carbonization, the salts in the intermediate products could be completely removed by water, which makes this synthesis much easier than other hard templating approaches. However, when the annealing temperature is increased to 800 °C, the salts would melt. As shown in Figure S3, when the intermediate was thermally annealed at 800 °C, the BET specific surface area of mesoporous carbon reaches 1205 $m^2\ g^{-1}$, which is much lower than that of MC. Moreover, the pore size calculated by the BJH method ranges from 2.0 to 50 nm with a wide distribution. The low surface area and the wide pore size distribution are both due to higher annealing temperature.

The electrochemical performance of MC as a supercapacitor electrode material was evaluated in two types of aqueous electrolytes in coin cells, i.e., 6 M KOH (Figure 5) and 1 M

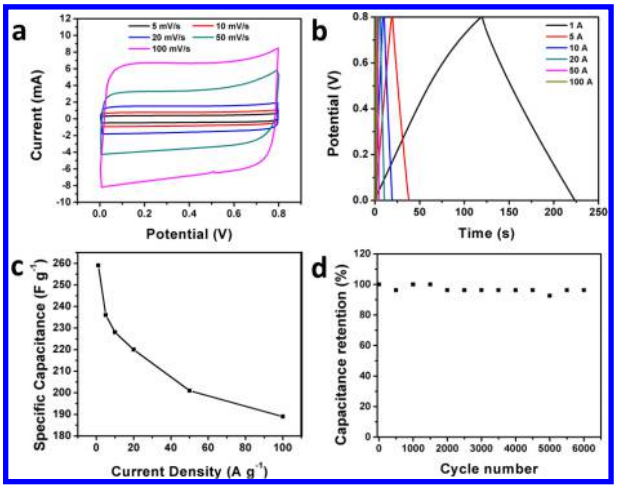

Figure 5. (a) CV curves of MC at different scan rates ranging from 5 to 100 mV s^{-1} in 6 M KOH aqueous solution. (b) Galvanostatic charge−discharge curves for MC at different current densities. (c) Specific capacitance of MC as a function of the scan rate. (d) Capacitance retention of MC measured at constant current density of 1 A g^{-1}.

Na_2SO_4 (Figure S5), with the optimal electrochemical performance achieved in the electrolyte of 6 M KOH. Cyclic voltammetry (CV) measurements were conducted at scan rates from 5 to 100 mV s^{-1} to test the rate stability of the electrodes (Figure 5a). Almost perfectly rectangular CV curves are observed at all scan rates, indicating low resistance and high power characteristics of the device. The galvanostatic charge/discharge curves for MC at multiple current densities are shown in Figure 5b. The specific capacitance of MC is 259, 236, 228, 220, 201, and 189 F g^{-1} at current densities of 1, 5, 10, 20, 50, and 100 A g^{-1}, respectively, which are calculated based on the slope of the discharge curves (as shown in Figure 5c). To the best of our knowledge, the capacitances of MC are among the highest values reported for the porous carbon materials (as shown in Table S1). The MC electrodes were also tested for 6000 charge/discharge cycles at 1 A g^{-1}. As shown in Figure 5d, 92% of the original capacitance is retained after 6000 cycles, indicating good cycle stability.

To gain insight into the capacitive performance of MC, electrochemical impedance spectroscopy (EIS) was performed in the frequency range of 10 mHz to 10 kHz at the open circuit voltage with a voltage amplitude of 5 mV. The squashed semicircle at high frequencies can be observed in the inset of Figure 6. It indicates the faradaic characteristic of charge transfer resistance at the electrode/electrolyte interface. The equivalent series resistance of the MC electrode is only 0.53 Ω (in term of the X-intercept of the Nyquist plots, as shown in Figure 6 inset), which indicates the high electrical conductivity. Besides, the short Warburg region indicates the short ion diffusion paths in the electrode due to the existence of the mesopore as an ion-buffering reservoir.[26] The almost vertical straight line at low frequencies features a nearly ideal double layer capacitive behavior.[27,28] The results above prove that MC is a suitable material to be used as the electrode of the electrochemical capacitor.

DOI: 10.1021/acsami.5b12164
ACS Appl. Mater. Interfaces 2016, 8, 6779−6783

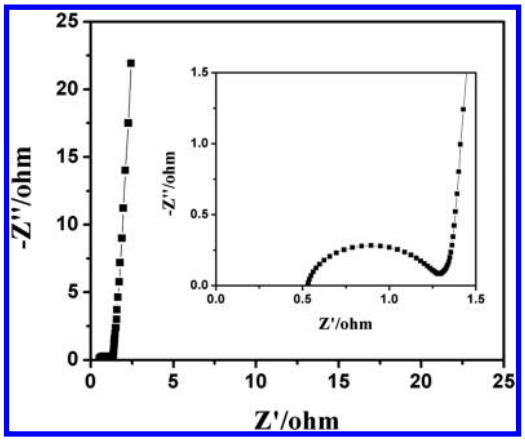

Figure 6. Nyquist plot of a typical MC electrode. The inset is an enlargement of the high-frequency region of the Nyquist plot.

In summary, we have demonstrated a facile synthesis procedure of the mesoporous carbon without any external templates. Upon the reduction of the CCl_4 precursor by NaK alloy, carbon and salt byproducts are simultaneously produced, precipitated and aggregated. The produced salts serve as templates for the formation of the mesoporous carbon, and can be easily removed by water, rather than harsh etchants, as is the case for other templates. The produced mesoporous carbon has a high BET surface area of 2012 $m^2\ g^{-1}$ and a narrow pore-size distribution, with an average pore diameter of 4 nm. As a supercapacitor electrode, this mesoporous carbon exhibits high specific capacitance (259 F g^{-1} at 1 A g^{-1}) and high rate stability (189 F g^{-1} at 100 A g^{-1}). As shown in Figure 5d, 92% of the original capacitance was retained after 6000 cycles, indicating good cycle stability. This process opens a new approach for the preparation of the mesoporous materials.

■ ASSOCIATED CONTENT

Supporting Information

The Supporting Information is available free of charge on the ACS Publications website at DOI: 10.1021/acsami.5b12164.

Detailed experimental procedures, as well as XRD, SEM, TEM, nitrogen adsorption/desorption isotherms, and other supplemental data (PDF)

■ AUTHOR INFORMATION

Corresponding Author

*E-mail: dwang@psu.edu.

Notes

The authors declare no competing financial interest.

■ ACKNOWLEDGMENTS

This work was supported by the Assistant Secretary for Energy Efficiency and Renewable Energy, Office of Vehicle Technologies of the U.S. Department of Energy under Contract Numbers of DE-EE0006447 and DE-EE0005475.

■ REFERENCES

(1) Meng, Y.; Gu, D.; Zhang, F. Q.; Shi, Y. F.; Yang, H. F.; Li, Z.; Yu, C. Z.; Tu, B.; Zhao, D. Y. Ordered Mesoporous Polymers and Homologous Carbon Frameworks: Amphiphilic Surfactant Templating and Direct Transformation. *Angew. Chem., Int. Ed.* **2005**, *44*, 7053−7059.

(2) Zhang, F. Q.; Meng, Y.; Gu, D.; Yan, Y.; Yu, C. Z.; Tu, B.; Zhao, D. Y. A Facile Aqueous Route to Synthesize Highly Ordered Mesoporous Polymers and Carbon Frameworks with *Ia3hd* Bicontinuous Cubic Structure. *J. Am. Chem. Soc.* **2005**, *127*, 13508−13509.

(3) Yang, J. P.; Zhai, Y. P.; Deng, Y. H.; Gu, D.; Li, Q.; Wu, Q. L.; Huang, Y.; Tu, B.; Zhao, D. Y. Direct Triblock-Copolymer-Templating Synthesis of Ordered Nitrogen-Containing Mesoporous Polymers. *J. Colloid Interface Sci.* **2010**, *342*, 579−585.

(4) Stein, A.; Wang, Z.; Fierke, M. A. Functionalization of Porous Carbon Materials with Designed Pore Architecture. *Adv. Mater.* **2009**, *21*, 265−293.

(5) Ryoo, R.; Joo, S. H.; Jun, S. Synthesis of Highly Ordered Carbon Molecular Sieves via Template-Mediated Structural Transformation. *J. Phys. Chem. B* **1999**, *103*, 7743−7746.

(6) Kim, T. W.; Park, I. S.; Ryoo, R. A Synthetic Route to Ordered Mesoporous Carbon Materials with Graphitic Pore Walls. *Angew. Chem., Int. Ed.* **2003**, *42*, 4375−4379.

(7) Al-Muhtaseb, S. A.; Ritter, J. A. Preparation and Properties of Resorcinol-Formaldehyde Organic and Carbon Gels. *Adv. Mater.* **2003**, *15*, 101−114.

(8) Yang, Z.; Xia, Y.; Sun, X.; Mokaya, R. Preparation and Hydrogen Storage Properties of Zeolite-Templated Carbon Materials Nanocast via Chemical Vapor Deposition: Effect of the Zeolite Template and Nitrogen Doping. *J. Phys. Chem. B* **2006**, *110*, 18424−18431.

(9) Zakhidov, A. A.; Baughman, R. H.; Iqbal, Z.; Cui, C.; Khayrullin, I. I.; Dantas, S. O.; Marti, J.; Ralchenko, V. G. Carbon Structures with Three-Dimensional Periodicity at Optical Wavelengths. *Science* **1998**, *282*, 897−901.

(10) Kim, C. H.; Lee, D. K.; Pinnavaia, T. J. Graphitic Mesostructured Carbon Prepared from Aromatic Precursors. *Langmuir* **2004**, *20*, 5157−5159.

(11) Xia, Y.; Mokaya, R. Ordered Mesoporous Carbon Hollow Spheres Nanocast Using Mesoporous Silica via Chemical Vapor Deposition. *Adv. Mater.* **2004**, *16*, 886−891.

(12) Xia, Y.; Mokaya, R. Generalized and Facile Synthesis Approach to N-Doped Highly Graphitic Mesoporous Carbon Materials. *Chem. Mater.* **2005**, *17*, 1553−1560.

(13) Li, Y. D.; Qian, Y. T.; Liao, H. W.; Ding, Y.; Yang, Li.; Xu, C. Y.; Li, F. Q.; Zhou, G. E. A Reduction-Pyrolysis-Catalysis Synthesis of Diamond. *Science* **1998**, *281*, 246−247.

(14) Liu, J. W.; Shao, M. W.; Tang, Q.; Chen, X. Y.; Liu, Z. P.; Qian, Y. T. A Medial-Reduction Route to Hollow Carbon Spheres. *Carbon* **2003**, *41*, 1682−1685.

(15) Xu, L. Q.; Zhang, W. Q.; Yang, Q.; Ding, Y. W.; Yu, W. C.; Qian, Y. T. A Novel Route to Hollow and Solid Carbon Spheres. *Carbon* **2005**, *43*, 1090−1092.

(16) Xie, Y. G.; Huang, Q. Z.; Huang, B. Y. Chemical Reactions between Calcium Carbide and Chlorohydrocarbon Used for the Synthesis of Carbon Spheres Containing Well-Ordered Graphite. *Carbon* **2010**, *48*, 2023−2029.

(17) Lu, A. H.; Schüth, F. Nanocasting: a Versatile Strategy for Creating Nanostructured Porous Materials. *Adv. Mater.* **2006**, *18*, 1793−1805.

(18) Chang, H.; Joo, S. H.; Pak, C. Synthesis and Characterization of Mesoporous Carbon for Fuel Cell Applications. *J. Mater. Chem.* **2007**, *17*, 3078−3088.

(19) Xu, B.; Peng, L.; Wang, G. Q.; Cao, G. P.; Wu, F. Easy Synthesis of Mesoporous Carbon Using Nano-$CaCO_3$ as Template. *Carbon* **2010**, *48*, 2377−2380.

(20) Guan, Z. R. X.; Liu, H.; Xu, B.; Hao, X.; Wang, Z. X.; Chen, L. Q. Gelatin-Pyrolyzed Mesoporous Carbon as a High-Performance Sodium-Storage Material. *J. Mater. Chem. A* **2015**, *3*, 7849−7854.

(21) Xu, B.; Duan, H.; Chu, M.; Cao, G. P.; Yang, Y. S. Facile Synthesis of Nitrogen-Doped Porous Carbon for Supercapacitors. *J. Mater. Chem. A* **2013**, *1*, 4565−4570.

(22) Xu, B.; Hou, S. S.; Chu, M.; Cao, G. P.; Yang, Y. S. An Activation-Free Method for Preparing Microporous Carbon by the Pyrolysis of Poly(vinylidene fluoride). *Carbon* **2010**, *48*, 2812−2814.

DOI: 10.1021/acsami.5b12164
ACS Appl. Mater. Interfaces 2016, 8, 6779−6783

(23) Dai, F.; Zai, J. T.; Yi, R.; Gordin, M. L.; Sohn, H. S.; Chen, S. R.; Wang, D. H. Bottom-Up Synthesis of High Surface Area Mesoporous Crystalline Silicon and Evaluation of Its Hydrogen Evolution Performance. *Nat. Commun.* **2014**, *5*, 3605−3615.
(24) Zhou, Q. Q.; Chen, X. Y.; Wang, B. An Activation-Free Protocol for Preparing Porous Carbon from Calcium Citrate and the Capacitive Performance. *Microporous Mesoporous Mater.* **2012**, *158*, 155−161.
(25) Liu, R. L.; Shi, Y. F.; Wan, Y.; Meng, Y.; Zhang, F. Q.; Gu, D.; Chen, Z. X.; Tu, B.; Zhao, D. Y. Triconstituent Co-Assembly to Ordered Mesostructured Polymer-Silica and Carbon-Silica Nanocomposites and Large-Pore Mesoporous Carbons with High Surface Areas. *J. Am. Chem. Soc.* **2006**, *128*, 11652−11662.
(26) Xiong, Z. Y.; Liao, C. L.; Wang, X. G. A Self-Assembled Macroporous Coagulation Graphene Network with High Specific Capacitance for Supercapacitor Applications. *J. Mater. Chem. A* **2014**, *2*, 19141−19144.
(27) Zhang, Z. J.; Chen, X. Y.; Xie, D. H.; Cai, P.; Liu, J. W. Temperature-Dependent Structure and Electrochemical Performance of Highly Nanoporous Carbon from Potassium Biphthalate and Magnesium Powder via a Template Carbonization Process. *J. Mater. Chem. A* **2014**, *2*, 9675−9683.
(28) Zhang, H. Q.; Hu, Z. Q.; Li, M.; Hu, L. W.; Jiao, S. Q. A High-Performance Supercapacitor Based on a Polythiophene/Multiwalled Carbon Nanotube Composite by Electropolymerization in an Ionic Liquid Microemulsion. *J. Mater. Chem. A* **2014**, *2*, 17024−17030.

DOI: 10.1021/acsami.5b12164
ACS Appl. Mater. Interfaces 2016, 8, 6779−6783